Noninvasive assessment of lymphatic impairment and interstitial protein accumulation using chemical exchange saturation transfer (CEST) MRI

Manus Donahue[1,2], Paula CM Donahue[3,4], Swati Rane[1], Megan K Strother[1], Allison O Scott[1], and Seth A Smith[1]

[1]*Radiology and Radiological Sciences, Vanderbilt University Medical Center, Nashville, TN, United States,* [2]*Physics and Astronomy, Vanderbilt University, Nashville, TN, United States,* [3]*Physical Medicine and Rehabilitation, Vanderbilt University Medical Center, Nashville, TN, United States,* [4]*Dayani Center for Health and Wellness, Nashville, TN, United States*

Target Audience: Researchers interested in breast cancer imaging, lymphatic functioning, and clinical applications of CEST

Purpose: *The overall goal of this work is to apply a custom CEST imaging approach to patients with, or at risk for, breast cancer treatment-related lymphedema (BCRL) to assess interstitial protein accumulation and lymphatic compromise.* Impairment of the lymphatics is known to reduce quality of life in some of the most crippling diseases of the 21st century, including lymphedema, obesity, cancer, and cardiovascular disease[1]. However, the lymphatics are not nearly as well understood as other bodily systems, largely owing to a lack of sensitive imaging technologies that can be applied using standard clinical equipment. Here, we apply APT CEST MRI[2] for the first time in patients with BCRL with the overall hypothesis that elevated interstitial protein accumulation will lead to an enhancement in the APT effect in a manner that depends spatially on limb involvement and extent of lymphedema severity. The long-term goal of this work is to demonstrate abilities to accurately record structural and functional observables of lymphatic dysfunction which can serve as trial end points for future clinical trials of lymphedema management therapies.

Methods: All subjects provided informed, written consent. Healthy controls (N=8; age=32-67 yrs) and BCRL patients (N=7; age=52-76 yrs) were scanned (3T; Philips) using dual-channel RF transmit/16-channel receive. Inclusion criteria: (Stage 0-2 BCRL) and lymph node resection. Additional information including circumferential arm measurements, medication regimen, duration since surgery, duration of radiation therapy, number of lymph nodes removed, breast reconstruction surgery, and handedness were recorded. CEST was performed with a 3D GRE with multi-shot EPI (factor=7), TR/TE=166/6.6 ms, slices=20, spatial resolution=3x3x10mm^3 (AP, RL, FH). CEST preparation was performed by applying a Gaussian windowed sinc saturation pulse with peak B_1 = 1 μT and duration=75 ms at offset frequencies $\Delta\omega$ = -6 to +6 ppm (0.25 ppm spacing). Structural MRI was also obtained (B_1 maps, T_1, T_2, DWIBS, and mDIXON). For analysis, CEST-weighted signals were normalized to a signal obtained at ± 80ppm (S_0) to generate a CEST z-spectrum. To correct for B_0 inhomogeneity, a single Lorentzian lineshape was fit to the CEST z-spectrum; the frequency offset corresponding to the Lorentzian minimum ($\Delta\omega_0$) was found and the z-spectrum was shifted such that $\Delta\omega_0$=0 ppm; both APT asymmetry (+3.5 ppm vs. -3.5 ppm) and the difference between the +3.5 ppm and magnitude of the Lorentzian at -3.5 ppm were recorded, with the latter "Lorentzian" approach reducing sensitivity to asymmetric MT effects. The primary objective was to assess the size of the APT effect in the affected and unaffected arms of patients and to contrast these values with asymmetry values observed in the right and left arms of control volunteers. A secondary aim was to assess whether variability in APT effect size could be explained by number of lymph nodes removed. To test the primary objective, an unpaired one-tailed t-test was applied between the asymmetry values in patients and controls, and a paired t-test was applied between APT effect sizes in the right versus left arms of controls or the affected versus unaffected arms of patients. To test the secondary objective, APT effect size was compared with the number of nodes removed using Pearson correlation testing.

Results and Discussion: Fig. 1 shows the location of the imaging on mDIXON (A) and DWIBS (B), representative B_1 maps and ROI (C), example asymmetry maps of a control and patient (D), corresponding z-spectra (E), and mean observed asymmetry (F). No significant difference between proton-weighted APT contrast in the right and left arms of healthy controls was observed. A trend (P=0.050) for an increase in APT effect size in the affected arms of patients was found, and variability between patients was consistent with number of nodes removed during resection (R=0.62; P=0.069; N=7). In terms of medical research, the lymphatic system is one of the most neglected bodily systems, which has resulted in an incomplete understanding of lymphatic functioning in health and disease. The purpose of this study was to evaluate for the first time whether noninvasive APT CEST MRI, which has demonstrated clinical potential in brain, liver, and breast applications, can be translated to the human lymphatic system to identify lymphatic dysfunction following breast cancer treatment. We observed that APT contrast could be observed in both healthy and BCRL patients. Also, relative to controls, increased APT asymmetry between healthy and lymphedematous arms was observed in patients with BCRL, and furthermore a strong trend for a relationship between APT effect size and number of lymph nodes removed was evident.

Conclusions: Elevated interstitial protein accumulation is a hallmark for lymphatic failure; these data support the ability of APT CEST to provide contrast consistent with lateralizing disease in patients with breast cancer treatment-related lymphedema, thereby motivating the further investigation of these and similar methods for evaluating lymphatic dysfunction.

References/Funding: [1]Mortimer PS et al. J Clin Invest. 2014 Mar 3;915-21.[2]Zhou J et al. Nat Med. 2003 Aug;1085-90. Funding: NIH/NINR 1R01NR015079-01.

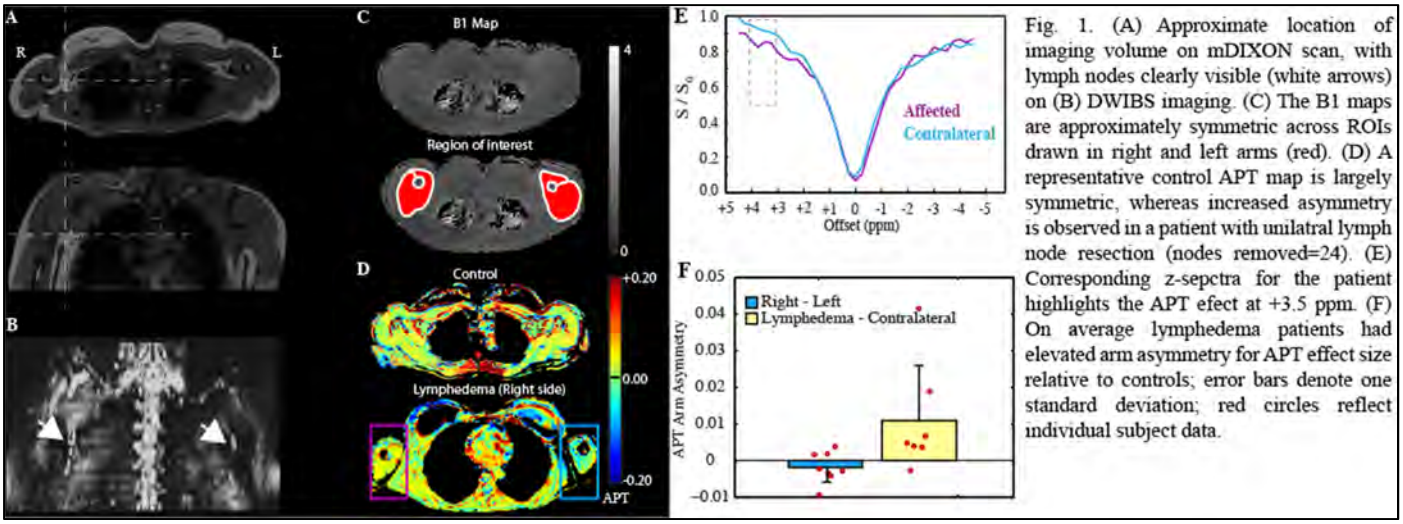

Fig. 1. (A) Approximate location of imaging volume on mDIXON scan, with lymph nodes clearly visible (white arrows) on (B) DWIBS imaging. (C) The B1 maps are approximately symmetric across ROIs drawn in right and left arms (red). (D) A representative control APT map is largely symmetric, whereas increased asymmetry is observed in a patient with unilatral lymph node resection (nodes removed=24). (E) Corresponding z-sepctra for the patient highlights the APT efect at +3.5 ppm. (F) On average lymphedema patients had elevated arm asymmetry for APT effect size relative to controls; error bars denote one standard deviation; red circles reflect individual subject data.